Spur Bevel Gearbox Fault Diagnosis Using Wavelet Packet Transform for Feature Extraction

Wentao Huang, Peilu Niu and Xiaojun Lu

Abstract Gear as an important transmission component in the production of modern industrial, used in all areas of production and life, its stable and reliable work has great social significance. In this paper, gear fault diagnosis based on wavelet packet for fault feature extraction has been proposed for gear fault detection and diagnosis. First, this paper analyzes the variations of gear fault vibration signal, using time-domain and frequency-domain sign attributes to characterize these gear vibration signal and then extract fault sign attributes by using wavelet packet. This paper introduces a kind of new method for wavelet de-noise, eliminating the problem of wavelet de-noise decompose level and de-noise threshold value selection, at the same time analysis a kind of wavelet packet transform method, eliminating the frequency and frequency band confusion, reducing the error in fault sign attribute extraction. At last, using fault simulation platform to simulate different conditions and different gear fault vibration signals. The results demonstrate that this method can accurately and reliably detect failure modes in a gearbox.

Keywords Fault diagnosis · Wavelet packet · Frequency aliasing

1 Introduction

Gearbox was an important component in industrial drives, its safe and reliable operation had great significance of industrial production. Used acceleration sensors can collect the vibration signal of the gearbox without disturb the gearbox normal working conditions, analysis the collected vibration acceleration signal to extracted the gearbox feature characteristics, so as to reflected the type of gearbox

W. Huang (✉) · P. Niu · X. Lu
School of Mechatronics Engineering, Harbin Institute of Technology, Harbin, China
e-mail: hwt@hit.edu.cn

Z. Wen and T. Li (eds.), *Practical Applications of Intelligent Systems*,
Advances in Intelligent Systems and Computing 279,
DOI: 10.1007/978-3-642-54927-4_15,

failure and fault degree. So we can take appropriate measures to minimize economic losses and improve production efficiency. Thus, the effective fault diagnosis method for the gear failure mode classification had important significance.

The primary concepts of wavelet analysis are dilation and translation. In 1983, Morlet proposed the concept of wavelets in the analysis of seismic data. In 1997, Xiong, Ramchandran, Herley, and Orchard proposed variable wavelet packet transform (WPT) algorithms based on a tree structure [1]. In 1999, Newland introduced the WPT in the engineering field, with several calculation methods and examples of his application in vibratory signal analysis [2]. In 2002, Zheng et al. published a gear fault diagnosis method based on a continuous wavelet transform and proposed a new concept of time-averaged wavelet spectrum for reducing the enormous operand [3]. In 2010, Lei et al. introduced a multidimensional hybrid intelligent method for gear fault diagnosis; a Hilbert transform, WPT, and empirical mode decomposition were used for gear multidimensional fault diagnosis [4]. In 2010, Zhou et al. introduced a gearbox fault diagnosis based on a redundant second-generation WPT; a second-generation WPT has a redundancy feature that is able to maintain time-invariant properties to increase the effectiveness of the information [5].

Many gear faults are partial failures, reflected in the change of partial information in the spectrum; therefore, gear fault diagnosis should focus on the partial information of the signal. The WPT can describe partial signal characteristics; a low-band WPT has low time resolution and high frequency resolution, whereas a high-frequency-band WPT had high time resolution and low frequency resolution. By further decomposing high-frequency information, the WPT can be more flexible in dividing signals. WPT provides an efficient and a reliable tool for the separation of the characteristic frequencies of mechanical failure and fault feature extraction.

In this paper, the proposed WPT is used for feature extraction. WPT analysis has an acute partial locked ability to extract feature information from the vibration signals. Using a WPT for partial gear vibration signal spectrum analysis or time-domain frequency attributes can help to detect gear failure. The single-node reconstruction of the wavelet coefficients can lead to the generation of other frequency components. If the gear signal spectrum analysis and the time—and frequency-domain sign attributes are false, they can affect the accuracy of the gear fault diagnosis. In this paper, we introduce an improved WP algorithm to eliminate the excess frequency components to ensure the accuracy of the partial attribute.

2 Data Acquisition Experiment

2.1 Experimental Setup

The gear fault forms are varied; in the same types of gear fault, the different fault degrees causing the form of gear vibration signals are not the same. To study the form of gear fault vibration in further detail, more accurate detection of the gear

Table 1 Gear wheel and pinion details

Parameters	Gear wheel	Pinion wheel
No. of teeth	27	18
Module	M2	M2
Pitch angle	56°19′	33°41′
Normal pressure angle	20°	20°
Material	Forged steel	Forged steel
Backlash tolerance (inches)	0.001–0.005	0.001–0.005
Pitch diameter (inches)	1.6875	1.125
Pinion bearing	NSK 6202 (2)	NSK 6202 (1)

fault is necessary. A mechanical failure simulator can be used to simulate different gear faults and provide analysis for the vibration signals of gear faults to obtain decision rules for the gear faults.

A variable speed DC motor (1 hp) with a speed of up to 6,000 rpm was used as the basic drive. A short shaft with a diameter of 0.75 inch was attached to the shaft of the motor through a flexible coupling; this scheme minimized the effects of misalignment and the transmission of vibrations from the motor.

The shaft was supported at its ends by two roller bearings. From this shaft, the motion was transmitted to the bevel gearbox via a belt drive. A torque attribute of 5 Nm was applied at the full load condition. Various defects were created in the pinion wheels, and the mating gear wheel was not disturbed. Gearbox vibration signals were obtained by mounting the accelerometer on the top of the gearbox.

2.2 Experimental Procedure

In this study, the gear pair details are listed in Table 1.

One wheel was new and assumed to be free from defects. In the other two pinion wheels, defects were created using an EDM to control the size of the defects. A piezoelectric acceleration sensor was mounted on the gearbox, and the electromagnetic spring loaded disc brake load was adjusted to 5 Nm. The DC motor speed adjusted the pinion shaft rotational speed to 11 Hz. The gearbox was initially run several times. The sampling frequency was 2,560 Hz, and the sample length was 2,048 for all data acquisition conditions. During the experiment, the normal pinion, tooth breakage pinion, and tooth surface wear pinion were used for data collection.

3 Wavelet Packet Transform Theory

3.1 Basic Concepts of WPT

For a discrete wavelet, the wavelet scale a and offset b must be discretized. To facilitate the calculation, a binary discrete of $a = 2^j$, $b = 2^j k$ was used, resulting in a binary discrete wavelet transform. The discrete wavelet transform at each level

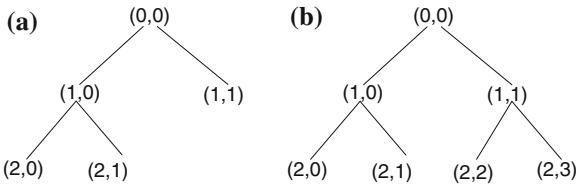

Fig. 1 Structure of the wavelet tree. **a** Discrete Wavelet Transform, **b** Wavelet packet transform

as the decomposition of a low-frequency sub-band (and no longer the decomposition of the details of the high-frequency sub-band) is illustrated in Fig. 1a. When further analysis of the high-frequency part was required, the discrete wavelet could not meet the requirements. Therefore, Coifman and Wickerhauser proposed the concept of WPT. The high-frequency part of each level was decomposed to meet the demand, as shown in Fig. 1b.

$$I_j^k = [-(k+1)\pi 2^{-j}, -k\pi 2^{-j}] \cup [k\pi 2^{-j}, (k+1)\pi 2^{-j}] \tag{1}$$

In actual production applications, the meaningful signal frequencies were positive. Therefore, the actual signal of the ith wavelet packet at the level-j $p_j^i(t)$ frequency band is the positive frequency portion, i.e.,

$$I_j^k = [k\pi 2^{-j}, (k+1)\pi 2^{-j}]. \tag{2}$$

Note that the frequency range of I_j^k was obtained under the assumption that the WPT filter was the ideal filter. However, this assumption was incorrect because the WPT filter did not have ideal cutoff characteristics. Therefore, in the single-node reconstruction algorithm, each sub-band contains some frequency components that do not belong to it, which generates frequency aliasing and causes artificial errors.

3.2 Frequency Aliasing

We next use an example to simulate the frequency aliasing. For the tooth breakage pinion, a sampling frequency of 2,560 Hz and a sample length of 2,048 were considered. The time- and frequency-domain waveforms of the tooth breakage are shown in Fig. 2. The signal was decomposed into three levels using a Db4 wavelet. The reconstructed signal spectrum waveform, whose node was reconstructed with a WPT, is presented in Fig. 3.

Based on WPT theory, the reconstructed signal of node (3, 0) only contains the information of (0, 160 Hz); node (3, 1) only contains the information of (160, 320 Hz); node (3, 2) only contains the information of (320, 480 Hz); and node (3, 3) only contains the information of (480, 640 Hz);

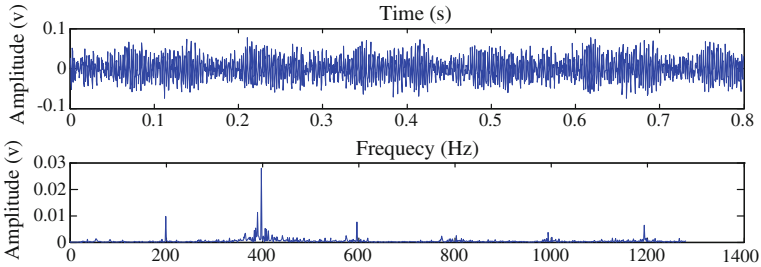

Fig. 2 Time- and frequency-domain waveforms of tooth breakage

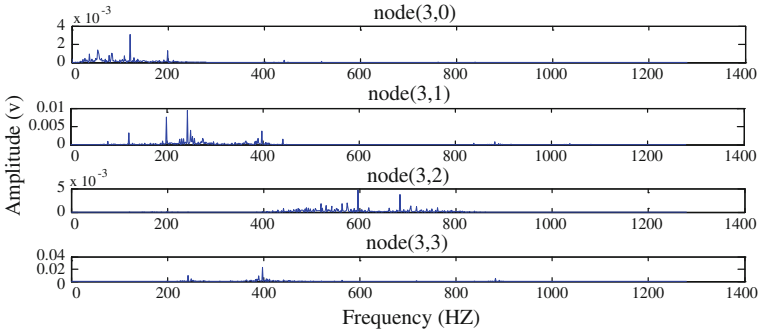

Fig. 3 Reconstructed signal spectrum waveform

Referring to Fig. 3, nodes (3, 0), (3, 1), (3, 2), and (3, 3) contain many other frequency components, resulting in a large amount of frequency aliasing. Node (3, 1) generated a pulse at 240 Hz, with a larger amplitude than that at 198 Hz. The initial signal did not generate a pulse frequency of 240 Hz, greatly affecting the accuracy of the gear fault diagnosis.

Based on WPT theory node (3, 2) only contains the information of (320, 480 Hz); node (3, 3) only contains the information of (480, 640 Hz); but referring to Fig. 3 node (3, 2) contains the information of (480, 640 Hz); and node (3, 3) contains the information of (320, 480 Hz), and nodes (3, 2) and (3, 3) had their frequency bands interleaved. The frequency band interleave becomes more complex as the level of decomposition increases. Analysis of the frequency aliasing indicates that the WPT frequency band interleave is regular; at each node, if the decomposition of the high frequency sub-band has a band interleave, the interleave of the low-level into the high-level will generate further interleave. According to the regular band interleave, reconstruction sorts the band interleave into the correct sequence to avoid a band interleave.

3.3 Eliminate Frequency Aliasing

WPT decomposition differs from discrete wavelet decomposition in that only the former decomposes the high-frequency portion of the signal. WPT filters do not have ideal characteristics; therefore, the detailed components of the level can generate frequency aliasing [6]. If the further decomposed detail parts are equivalent to the decomposed false signals, then reconstructing these parts also reconstructs false ingredients [7].

Frequency aliasing is inherent in WPT decomposition algorithms. To eliminate frequency aliasing, one must proceed with three basic operations of the algorithm. To improve the convolution of the wavelet packet filters, interval point sampling and interval dot zero insertion must be used to eliminate frequency aliasing.

Using a WPT for gearbox fault diagnosis generated the other frequency components due to frequency aliasing. In the spectral analysis, the node (3, 1) in Fig. 3 generated an additional pulse shock, causing the testing personnel to generate a judgment error. For gear sign attribute extraction, the extracted attributes also contained many false components, which influenced the accuracy of the gear fault diagnosis. Therefore, eliminate the single node reconstruct frequency aliasing was of great significance. Concrete steps to achieve the improved algorithm were as follows [8]:

- Each wavelet coefficient performs a Fourier transform after filter convolution.
- The superfluous portion of the spectrum is set to zero and then performs an inverse Fourier transform of the spectrum.
- The results of the inverse transformation replace the results of wavelet filter convolution. Wavelet packet decomposition and reconstruction continues.
- The interleaved band is adjusted to obtain the correct band of the spectrum signal.

Using the improved WPT algorithm in the above example, the reconstructed signal spectrum waveform is shown in Fig. 4.

Contrasting Fig. 3 with Fig. 4, one can observe that the improved WPT algorithm effectively eliminated the frequency aliasing. By adjusting the wavelet subband dislocation sequence, the sequence interleave problems were resolved.

The WPT algorithm achieved a reconstructed signal of each node that only contained the signal of the theoretical frequency domain without any additional frequency components. However, the nonideal cutoff characteristic of the wavelet filters caused a leakage of signal energy, therefore decreasing the amplitude of the reconstructed signal in each node.

The improved wavelet packet algorithm led each node to contain only the theoretical frequency information. The characteristics of the nonideal wavelet filter generated other frequency components. Applying this wavelet node information to the fault diagnosis could accurately express the respective frequency components, which can significantly increase the accuracy of fault diagnosis.

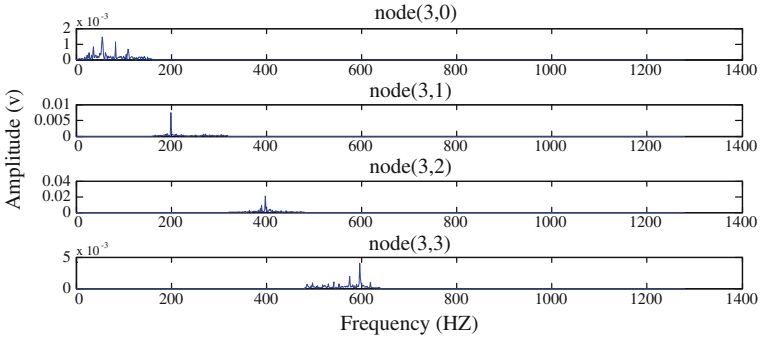

Fig. 4 Reconstructed signal spectrum waveforms using the improved algorithm

4 Fault Feature Extraction

Adjusting the rotational speed of the motor changed the pinion shaft speed to 11 Hz, resulting in a gear mesh frequency of 198 Hz. The gear vibration signal was extracted when the speed was stable. Figures 5, 6, and 7 present the time- and frequency-domain spectrum waveform of the normal pinion, tooth breakage pinion, and tooth wear pinion, respectively. These figures illustrate that the three pinion states are mainly distributed in the pinion mesh frequency at the second and third harmonics. The extracted signal features are $f = f_m = 198$ Hz, $f = 2\,f_m = 396$ Hz, and $f = 3\,f_m = 594$ Hz.

For the signal with a sampling frequency of 2,560 Hz, the WPT wavelet node (3, 0) contains a frequency component of (0, 160 Hz), node (3, 1) contains a frequency component of (160 Hz, 320 Hz), node (3, 2) contains a frequency component of (320 Hz, 480 Hz), and node (3, 3) contains a frequency component of (480 Hz, 640 Hz). We extracted features from the WPT decomposition and reconstruction nodes (3, 1), (3, 2), and (3, 3) for pinion fault diagnosis.

Using the WPT for single-node reconstruction, the single-node reconstruction time-domain waveform for the normal pinion, tooth breakage pinion, and tooth wear pinion are shown in Figs. 8, 9, and 10, respectively.

In this paper, we selected nondimensional time-domain parameters to characterize the gear state.

$$\text{Kurtosis}: \qquad x_q = \frac{1}{N}\sum_{i=0}^{N-1} x_i^4 / x_a^2 - 3 \tag{3}$$

$$\text{Waveform indicators}: \; K = x_{\text{rms}}/x' \tag{4}$$

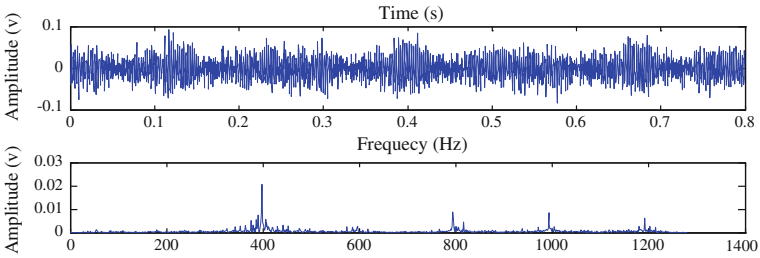

Fig. 5 Normal pinion time- and frequency-domain spectrum waveform

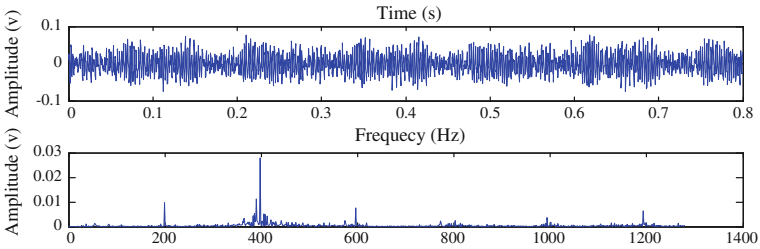

Fig. 6 Tooth breakage time- and frequency-domain spectrum waveform

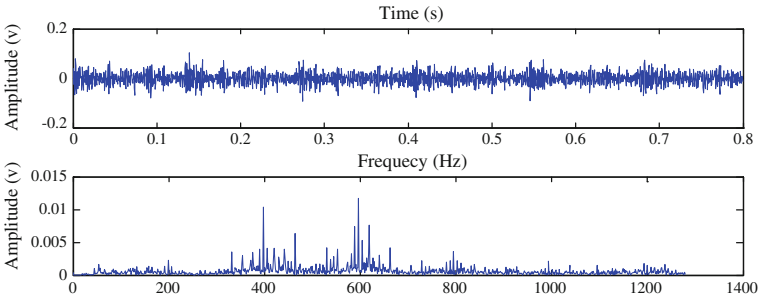

Fig. 7 Tooth wear pinion time- and frequency-domain spectrum waveform

$$\text{Peak indicators}: \quad C = x_p / x_{\text{rms}} \tag{5}$$

$$\text{Pulse indicators}: \quad I = x_p / x' \tag{6}$$

$$\text{Margin index}: \quad L = x_p / x_r \tag{7}$$

Here, x_a is the mean square value, $x_a = \sum_{i=1}^{N} x_i^2 / N$; x' is the average amplitude, $x' = \sum_{i=1}^{N} x_i / N$; x_{rms} is the mean square amplitude; $x_{\text{rms}} = \sqrt{x_a}$; x_p is the peak value, $x_p = \max(x_i)$; and x_r is the amplitude of the square root, $x_r = (\sum_{i=1}^{N} \sqrt{|x_i|} / N)^2$.

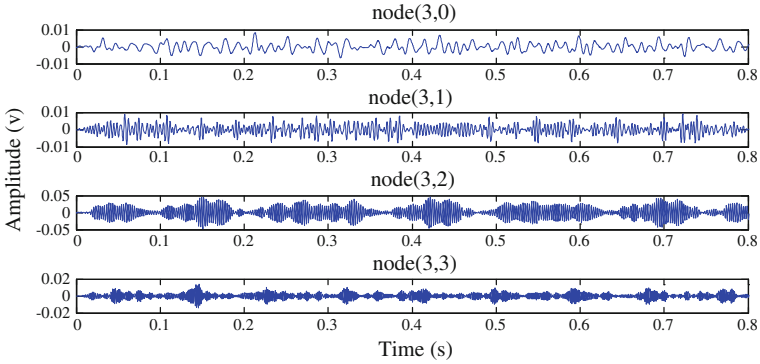

Fig. 8 Normal pinion single-node reconstruction time-domain waveform

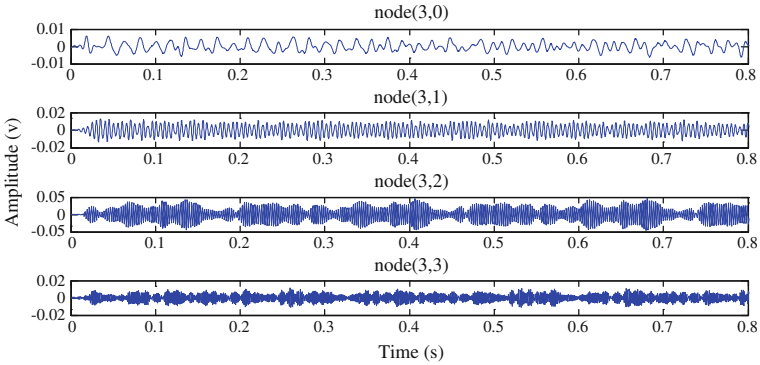

Fig. 9 Tooth breakage single-node reconstruction time-domain waveform

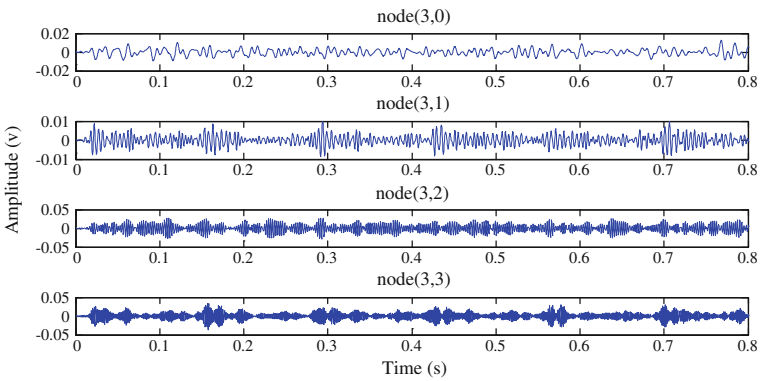

Fig. 10 Tooth wear single-node reconstruction time-domain waveform

In the selection time domain, we selected the sum of the node frequency-domain amplitude spectrum G to characterize the gear state.

$$G = \sum_{i=1}^{N} (|y_i| \times 2/N) \tag{8}$$

Here, y_i is the FFT of x_i.

The kurtosis indices of nodes (3, 1), (3, 2), and (3, 3) are defined as xq_1, xq_2, and xq_3, respectively; other indicators are also defined with this method. We extracted 18 total attribute signs to characterize the state of the pinion, namely, [xq_1, xq_2, xq_3, K_1, K_2, K_3, C_1, C_2, C_3, I_1, I_2, I_3, L_1, L_2, L_3, G_1, G_2, G_3]. Normal, tooth breakage and tooth wear were the three gear states; we sampled each state for 40 datasets, totaling 120 datasets as the raw data for fault diagnosis.

5 Discussion and Conclusion

In this paper, we did a full analysis and research on gear fault detection based on fault feature extraction using wavelet packet. First we analyzed gear dynamics, discussed the types of gear vibration signal. Based on the actual fault signal, we obtained different forms of gear fault vibration signal. According to the form of gear vibration signal chose appropriate characteristic parameters to describe the gear faults. Second, this paper introduces a kind of new method for wavelet de-noise, eliminating the problem of wavelet de-noise decompose level and de-noise threshold value selection, at the same time analysis a kind of wavelet packet transform method, eliminating the frequency and frequency band confusion, reducing the error in fault sign attribute extraction. Finally, through analyzing different gear fault vibration signal in different conditions; combined with theoretical analysis, extract symptom attributes by using signal wavelet packet analysis, so as to carry out the gear fault detection and diagnosis.

Acknowledgment This research is supported by the National Natural Science Foundation of China (51175102).

References

1. Xiong Z, Ramchandran K, Herley C, Orchard MT (1977) Flexible tree-structured signal expansions using time-varying wavelet packets. IEEE Trans Signal Process 45:333–345
2. Newland DE (1999) Ridge and phase identification in the frequency analysis of transient signals by harmonic Wavelets. J Vibr Acoust Trans ASME 121:149–155
3. Zheng H, Li Z, Chen X (2002) Gear fault diagnosis based on continuous wavelet transforms. Mech Syst Signal Process 16:447–457

4. Lei Y, Zuo MJ, He Z, Zi Y (2010) A multidimensional hybrid intelligent method for gear fault diagnosis. Expert Syst Appl 37:1419–1430
5. Zhou R, Bao W, Li N, Huang X, Yu D (2010) Mechanical equipment fault diagnosis based on redundant second generation wavelet packet transform. Digit Signal Proc 20:276–288
6. Pawlak Z (1982) Rough set. Int J Comput Inform Sci 11:341–356
7. Kryszkiewicz M (1998) Rough set to incomplete information systems. Inf Sci 112:39–49
8. Tay FEH, Shen LX (2003) Fault diagnosis based on rough set theory. Eng Appl Artif Intell 16:39–43